



Deliverable D11.4: Report on closure results between the measurements of absorption coefficient and black carbon concentration

R.L. Modini¹, N. Bukowiecki¹, B. Wehner², T., M. Müller², T. Tuch², S. Pfeifer², J.S. Henzing³, M. M. Moerman³, P. Fetfatzis⁴, M. Gini⁴, K. Eleftheriadis⁴, M. Zanatta⁵, A. Herber⁵, P. Laj⁶, A. Marinoni⁷, D. Orsini⁷, P. Cristofanelli⁷, S. Gilardoni⁷, and M. Gysel¹

¹ Laboratory of Atmospheric Chemistry, Paul Scherrer Institute, Villigen, CH-5232, Switzerland

² Leibniz-Institute for Tropospheric Research, Leipzig, Germany

³ Netherlands Organization for Applied Scientific Research (TNO), Utrecht, the Netherlands

⁴ National Centre of Scientific Research "DEMOKRITOS", Athens, Greece

⁵ Alfred Wegener Institute, Helmholtz Centre for Polar and Marine Research, Bremerhaven, Germany

⁶ Université Grenoble-Alpes, CNRS, Institut des Geosciences pour l'Environnement (IGE), Grenoble, France

⁷ National Research Council of Italy, Institute for Atmospheric Sciences and Climate, 40129 Bologna, Italy

Work package no	WP11: Improving the accuracy of aerosol light absorption determinations
Deliverable no.	D11.4: Report on closure results between the measurements of absorption coefficient and black carbon concentration
Lead beneficiary	
Deliverable type	<input checked="" type="checkbox"/> R (Document, report) <input type="checkbox"/> DEC (Websites, patent fillings, videos, etc.) <input type="checkbox"/> OTHER: please specify
Dissemination level	<input checked="" type="checkbox"/> PU (public) <input type="checkbox"/> CO (confidential, only for members of the Consortium, incl Commission)
Estimated delivery date	Month 42
Actual delivery date	31/10/2018
Version	
Comments	

Contents

1	Introduction.....	2
2	Absorption coefficient results	6
2.1	The CAPS PM _{ss,a}	6
2.1.1	Description of the CAPS PM _{ss,a} as an absorption photometer.....	6
2.1.2	Cross-calibration of CAPS PM _{ss,a} scattering coefficients	7
2.1.3	Truncation correction of CAPS PM _{ss,a} scattering coefficients	9
2.1.4	Closure between scattering coefficients measured in the field by CAPS PM _{ss,a} and other nephelometers	11
2.1.5	Absolute calibration of CAPS PM _{ss,a} extinction coefficients.....	12
2.1.6	Closure between extinction coefficients measured in the field by CAPS PM _{ss,a} and other instruments.....	13
2.1.7	Closure between absorption coefficients measured in the field by CAPS PM _{ss,a} and other instruments.....	14
2.2	The photoacoustic extinciometer (PAX).....	16
2.2.1	Description of the instrument	16
2.2.2	Closure between absorption coefficients measured in the field by the PAX and other instruments.....	16
2.3	Summary of ambient absorption coefficients and outlook for the future	17
3	BC mass concentration results.....	17
3.1	Closure between BC mass concentrations measured in the field by the SP2 and thermal-optical methods.....	17
3.2	The next generation SP2 instrument: the extended range SP2 (SP2-XR)	18
4	Outlook: MAC _{BC} measurements.....	19
5	References.....	20

1 Introduction

Light absorption is a key climate-relevant aerosol property of particular importance for aerosol-radiation and aerosol-cloud interactions (IPCC, 2013). Specifically, aerosol absorption can (i) directly modify the global radiation budget, (ii) indirectly modify cloud properties and abundance (e.g. Bond et al., 2013) and (iii) modify the atmospheric stability in the boundary layer and free troposphere (e.g. Babu et al., 2011). However, the magnitude of absorption on the global scale is subject to considerable uncertainties for aerosol particles of both anthropogenic and natural origin (IPCC, 2013). While the aerosol optical depth (AOD) and aerosol particle size distribution are relatively well-constrained from measurements, uncertainties in the single scattering albedo (SSA) (e.g. Loeb and Su, 2010), and especially the vertical profile of the black carbon (BC) concentration (e.g. Zarzycki and Bond, 2010), contribute significantly to the overall uncertainties of the aerosol radiative effect. More specifically, the light absorption of BC,

which is the predominant anthropogenic absorber, is most probably poorly represented in atmospheric models due to the variability of the BC mass absorption cross section (MAC_{BC}), which depends on a wide variety of additional variables such as the size, morphology and mixing state of the particles, amount of scattering material, and relative humidity. Furthermore, the absorption of natural aerosols such as mineral dust, is subject to considerable uncertainties as well since the imaginary part of the refractive index depends crucially on the dust mineralogical phase (e.g. Petzold et al., 2009), affecting the variability of dust absorption globally and resulting in diverse assumptions in atmospheric models and satellite retrievals.

The novel instrumentation operated in ACTRIS can serve for a comprehensive absorption characterization for anthropogenic and natural aerosols, utilizing urban and remote stations of the network. In-situ instrumentation and methods can be used to assess the relationship between absorption and BC concentration at representative sites. The vertical distribution of the absorption coefficient and the SSA, crucial for climatic applications, can be retrieved by both in-situ airborne methods and remote sensing techniques. Closure studies between remote sensing retrievals and in-situ measurements can lead to a better aerosol absorption characterization with respect to the aerosol type and contribute to reducing the related uncertainties. Finally, multi-wavelength absorption in-situ reference methods as well as retrievals can significantly add to improving aerosol characterization, speciation, and source apportionment.

JRA1 (WP11) is a joint research activity; its outcome is expected to contribute to quantitative and qualitative improvements of the services provided by the infrastructure. It involves field measurements with subsequent data analysis, but also the re-analysis of data collected in ACTRIS FP7 and other project frameworks. The motivation, goals and activities for JRA1 are summarized in Figure 1.

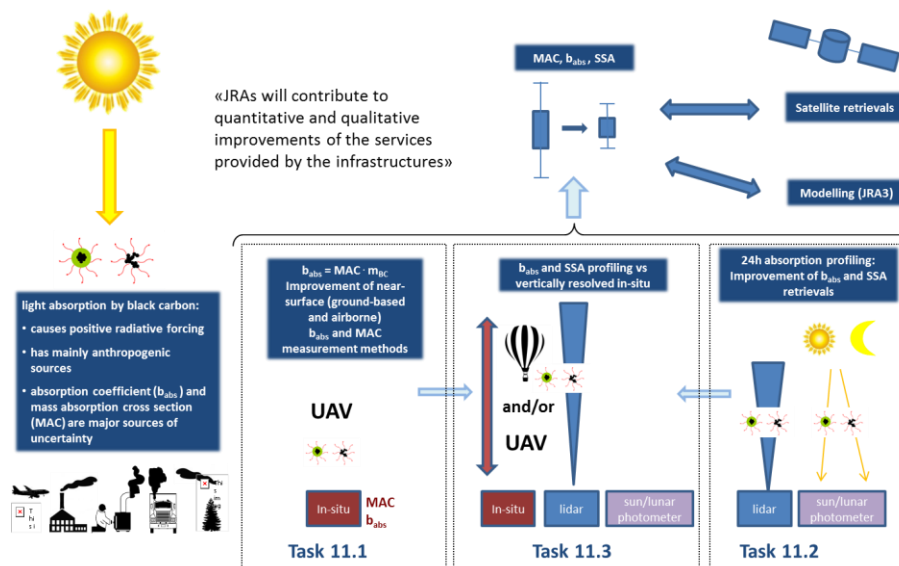


Figure 1: Motivations, goals and activities of JRA1 (WP11)

As part of Task 11.1 on the *in situ* determination of aerosol light absorption, a number of field campaigns were performed to intercompare different methods for measuring the two parameters required to calculate mass absorption cross section (MAC_{BC}) values for black carbon (BC): aerosol light absorption and BC mass. It is important to develop the capability to measure these parameters accurately and routinely in the field in order to investigate and compare MAC_{BC} values measured across different studies, and to elucidate the dependence of MAC_{BC} value on the size, morphology, and mixing state of ambient BC particles. This report details the results of the intercomparison studies and discusses the extent to which closure was achieved between the different measurements of BC mass and light

absorption. The report is a precursor to Deliverable D11.6, which will be an additional report evaluating MAC_{BC} measurements from different field sites, with the goal of investigating source-specific light absorption characteristics.

The side by side intercomparison of different absorption instruments has two aspects. On the one hand the results of this intercomparison are used as input towards the ongoing harmonization and standardization efforts made for absorption monitors that have existed for a long time (MAAP, aethalometers AE31 and AE33); on the other hand the existing monitors are compared to newly available instruments like the CAPS monitors (CAPS PM_{ssa}, CAPS PM_{ex}, PAX):

- The Multi-Angle Absorption Photometer (MAAP) determines the online light absorption of a PM deposit on a filter by simultaneously measuring the transmissivity and reflectivity of the filter at multiple angles. These measurements are inverted to yield the absorption coefficient by applying a radiative transfer model (Petzold and Schönlinner, 2004). The MAAP has been extensively tested and evaluated (Müller et al., 2011a; Slowik et al., 2007) and is considered an absorption standard. However, the MAAP only measures absorption at a single wavelength (637 nm), so knowledge of the wavelength-dependence of absorption is required to infer absorption at other wavelengths. As of 2017, the production of the MAAP has been discontinued.
- The dual-spot Aethalometer (AE33, Magee Inc) (Drinovec et al., 2015) infers light absorption online based on the transmissivity of a PM deposit on a filter. The AE33 has been shown to provide reliable measurements of the spectral dependence of the absorption coefficient in the wavelength range from 370 nm to 950 nm. However, it does not provide accurate values of the absolute absorption coefficients, due to a scaling factor in the data analysis approach which depends on other aerosol properties.
- The CAPS PM_{ex} (Aerodyne Inc.)(Massoli et al., 2010) is an extinction monitor. The three deployed units operated at 450, 530, and 630 nm. Extinction is measured by cavity attenuated phase shift spectroscopy, which determines light decay in an optical cavity and is theoretically calibration-free (Massoli et al., 2010), except for a factor which accounts for the effective detection volume. The light source is a cost-effective LED, so this instrument would be viable for a large-scale monitoring network. The three deployed units operated at 450, 630, and 780 nm.
- The CAPS PM_{ssa} (Aerodyne Inc.) measures absorption via the extinction-minus-scattering (EMS) method at a single wavelength. Scattering is measured independently by an integrating-sphere-type integrating nephelometer surrounding the CAPS optical cavity. Further details of the instrument have been provided in an initial technical paper (Onasch et al., 2015).
- The PAX (Photoacoustic extinctionsmeter, Aerodyne Inc.) provides a direct in-situ measurement of absorption coefficient using photo-acoustic spectroscopy. Recent progress improved the sensitivity of such instruments to a range where they become suitable for atmospheric measurements, at least in more polluted environments. It includes an integrating nephelometer, which makes particle based calibration (in addition to gas based) calibration possible and provides aerosol extinction and SSA by combining these two measurements.

The two main direct techniques currently used to measure aerosol BC mass in the atmosphere are evolved gas analysis and laser-induced incandescence. Additional analytical methods and related terminology are discussed by Petzold et al., (2013b).

Evolved gas analysis involves the detection of carbon desorbed from an aerosol-laden filter and converted to CO₂ as a function of temperature in different types of analytical atmospheres. Total carbon (TC) detected in this manner represents the sum of organic carbon (OC) and elemental carbon (EC). EC represents the thermally stable fraction of BC. Different heating protocols are used to optimally discriminate between OC and EC for different types of aerosol samples (e.g. the EUSAAR_2, IMPROVE, NIOSH protocols). However, pyrolysis of OC can lead to its incorrect classification as EC in thermal-only

based methods. The transmission or reflectance of laser light incident on a sample can be monitored to detect the fraction of pyrolytic carbon and correct for this potential systematic bias – these are known as thermal-optical transmittance (TOT) or reflectance (TOR) methods. The thermal-optical EUSAAR protocol has been developed for Europe (Cavalli et al., 2010) and is the standard method for measuring EC concentrations in the ACTRIS network.

The Single-Particle Soot Photometer (SP2) quantifies black carbon mass at the single-particle level using continuous wave laser-induced incandescence (LII) (Laborde et al., 2012; Schwarz et al., 2010). BC-containing particles are heated up to the boiling point of BC at around 4'000 °C and the operationally defined “refractory black carbon mass” (rBC mass) is quantified by detection of the thermal radiation emitted by the incandescent BC. A key strength of the SP2 is that it detects rBC mass without interferences from other internally or externally mixed particulate matter (Moteki and Kondo, 2007). However, empirical calibration is required to infer rBC mass from the thermal radiation. Furthermore, the traditional SP2 is more a research grade than a monitoring type instrument concerning the complexity of operation and data analysis. Very recently a simplified version, the SP2-XR was introduced, which might have the potential to be operated in monitoring networks. In this report we also include some first intercomparisons of the SP2-XR with the traditional SP2.

Extensive intercomparison exercises between different methods to measure absorption coefficient and black carbon mass have been performed during a row of dedicated field campaigns, see

Table 1.

- From May 4 until July 10 2015 the Melpitz column campaign (“MELCOL”) was performed at the ACTRIS site Melpitz (Germany), 40 km north east of Leipzig. The campaign was led by TROPOS with contributions from PSI, Universities of Bayreuth, Braunschweig, Darmstadt, and Tübingen as well as from the German Weather Service (DWD). The main goal of the campaign was the detailed characterization of the column above the Melpitz site in terms of aerosol particles, their radiative properties and meteorological parameters. In overview, the measurements showed that the atmosphere at the Melpitz ground site in summer 2015 was relatively clean. Both extinction and absorption coefficients were low, especially absorption.
- The Athens smog ACTRIS JRA1 campaign focused on the alterations of the absorption of the man-made aerosol pollution in the urban environment of Athens due to economic crisis, concentrating on the “smog” phenomenon caused by wood-burning for heating purposes. The campaign took place from 15th of December 2015 until 29th of February 2016 at the Thissio site, Athens, Greece. Specifically, the aerosol characterization was established by ground-based active/passive remote sensing techniques, surface in-situ measurements and airborne (UAV) observations. A description of the campaign, along with an overview of all the acquired measurements is available at the campaign website: <http://actris-athens.eu/>.
- From 9 September to 30 September a campaign was performed in Cabauw, The Netherlands, jointly with the CINDI-2 campaign (Cabauw Intercomparison of Nitrogen Dioxide Measuring Instruments 2), It was organized by TNO/UU and with participation of PSI, CNRS, IDAEA-CSIC and NCSR Demokritos. The atmospheric conditions were favourable with respect to the task goals.
- In February and March 2017, TROPOS organized the second “MELCOL” campaign in Melpitz, Germany, with participation of PSI, University of Leipzig and AWI. This campaign was a repetition of the first MELCOL campaign in June 2015, which suffered from too low ambient aerosol concentrations due to unfavourable meteorological conditions. During the second campaign concentrations were sufficiently high to use the collected data for the foreseen data analysis within this task.
- In July 2017, the “Monte Cimone ACTRIS2 JRA1” campaign took place at three different sites around Bologna, Italy, with a major goal of assessing the processes affecting the variability of the MAC value. The campaign was organized by CNR-ISAC and with participation of PSI, NCSR

Demokritos, JRC, Jožef Stefan Institute, IGE, FMI, Michigan Technological University, FTMC, Milan University and the companies AERODYNE and ALA (Advanced LIDAR Applications). Concentrations of absorbing aerosol species were generally sufficiently high.

Table 1: Summary of the absorption coefficient and BC mass concentration measurements performed during the JRA1 field campaigns dedicated to Task 11.1

Field campaign	Dates	Coordinator (institute)	In situ measurements	
			Absorption coefficient	BC mass concentration
Melpitz summer	May/June 2015	Birgit Wehner (TROPOS)	CAPS PM _{ss} a at 450, 630 and 780 nm (PSI), MAAP (637 nm), AE33 (7λ) + CAPS PM _{ex} for extinction at 450, 530, and 660 nm.	rBC: SP2 (PSI) EC: EUSAAR TOT and TOR
Athens	Dec 2015–Feb 2016	Vassilis Amiridis (NOA)	CAPS PM _{ss} a at 630 and 450 nm (NCSR Demokritos, PSI), MAAP (637 nm), AE33 (7λ)	EC
Cabauw	Sep/Oct 2016	Bas Henzing (TNO)	CAPS PM _{ss} a at 530 and 630 nm (NCSR Demokritos, PSI), MAAP (637 nm), AE33 (7λ)	rBC: SP2 (PSI, LGGE) EC: EUSAAR and TNO
Melpitz winter	Jan/Feb 2017	Birgit Wehner (TROPOS)	CAPS PM _{ss} a at 450, 630 and 780 nm (PSI), PAX (PSI), MAAP (637 nm), AE33 (7λ) + CAPS PM _{ex} for extinction at 450, 530, and 660 nm.	rBC: SP2 (AWI), SP2-XR (AWI) EC: EUSAAR TOT and TOR
Bologna	July 2017	Angela Marinoni (CNR)	CAPS PM _{ss} a 450, 630 and 780 nm (NCSR Demokritos, Aerodyne, PSI), MAAP (637 nm), AE33 (7λ)	rBC: SP2 (PSI) EC: EUSAAR

2 Absorption coefficient results

2.1 The CAPS PM_{ss}a

2.1.1 Description of the CAPS PM_{ss}a as an absorption photometer

The CAPS PM_{ssa} measures aerosol absorption coefficients (b_{abs}) by taking the difference of extinction (b_{ext}) and scattering (b_{sca}) coefficients measured for the same volume of air (extinction-minus-scattering, EMS). Uncertainty in absorption coefficients measured by the EMS method can be very large when scattering coefficients are only slightly smaller than extinction coefficients (i.e. at high SSA values) since two large numbers are being subtracted to produce a small number (subtractive cancellation error). For this reason, uncertainties in the underlying measurements of scattering and extinction must be well understood and minimised if the CAPS PM_{ssa} is to be an effective, stand-alone absorption photometer.

2.1.2 Cross-calibration of CAPS PM_{ssa} scattering coefficients

Scattering coefficients are measured in the CAPS PM_{ssa} by an integrating-sphere-type integrating nephelometer surrounding the optical cavity. The scattering signal must be calibrated. The technical paper introducing the instrument (Onasch et al., 2015) described a method for cross-calibrating the scattering signal against the independent extinction channel (which is theoretically 'calibration-free') using purely scattering particles (i.e. SSA = 1) such as ammonium sulphate or polystyrene latex (PSL) spheres. The results of such a 'particle' calibration performed during the Cabauw field campaign with a 530 nm PM_{ssa} monitor are displayed in Figure 2a). A differential mobility analyser (DMA) was used to size select ammonium sulphate particles with mobility diameters between 100-250 nm before they were measured by the PM_{ssa} monitor. No size dependence is visible in the ratio of scattering to extinction indicating that truncation of the scattering signal (see Section 2.1.3) does not affect the calibration over the examined size range. The tight linear fit to the measurements (using all particle sizes) indicates a high degree of linearity between extinction and scattering measured by the CAPS PM_{ssa} at atmospherically-relevant extinction levels (< 200 Mm⁻¹). The cross-calibration factor is taken as the slope of this linear fit.

A method for cross-calibrating the CAPS PM_{ssa} with gases was also investigated in the JRA1 field campaigns. An example result of such a calibration performed for a 450 nm PM_{ssa} monitor during the Melpitz summer campaign is shown in Figure 2b). The gas cross-calibration method is based on the well-known span gas calibration performed for integrating nephelometers (e.g. Anderson et al., 1996). Specifically, particle-free gases with low scattering coefficient (in this case filtered air) and higher scattering coefficient (in this case CO₂) are sampled by the monitor. A linear fit between the scattering and extinction measurements of the two gases represents the cross-calibration. The gas cross-calibration method relies on the assumption of linearity between scattering and extinction in the CAPS PM_{ssa} if only two gases are used, and it covers a much smaller range of extinction values than is achievable with the particle method. In addition, it was found that the PM_{ssa} monitors required very long periods of time (~hrs) to adjust and stabilize when filled with different gases. Therefore the gas calibrations generally took far longer than the particle calibrations to perform. Furthermore, a gas-based cross-calibration requires additional corrections to account for the fact that the relevant path length for the extinction differs between gas and particle measurements. For these reasons, it is recommended to perform particle based cross-calibration using aerosol particles with size parameters in the Rayleigh regime.

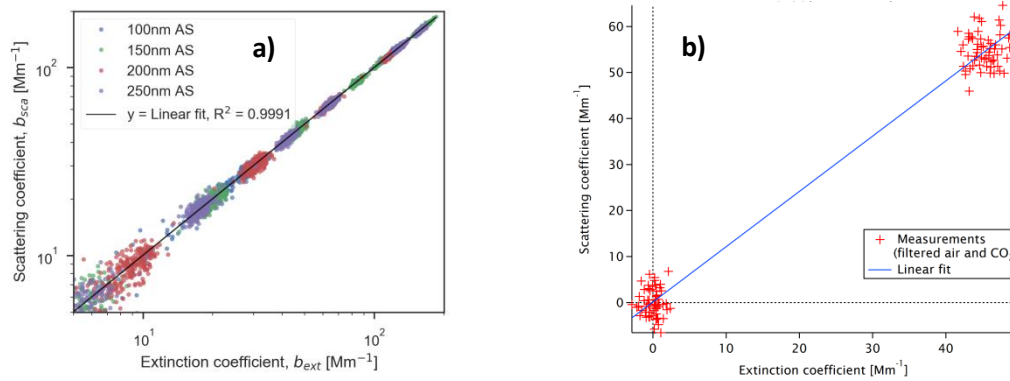


Figure 2: CAPS PMssa scattering to extinction cross-calibrations: **a)** a particle calibration for a 530 nm PMssa monitor (PSI) performed during the Cabauw campaign with ammonium sulphate (AS) particles of different DMA-selected mobility diameters that are indicated in the legend, and **b)** a gas calibration for a 450 nm PMssa monitor (PSI) performed during the Melpitz summer campaign with filtered air (as zero gas) and CO₂. Data points are shown on native time resolution (1s).

The stability of CAPS PMssa cross-calibration factors was also investigated. Initial results for PSI's 780 nm monitor obtained before, during, and after the Melpitz summer campaign were highly variable, with cross-calibration factors (measured by both gas and particle calibration methods) varying by $\pm 10\text{-}15\%$ (Figure 3). Further, shorter-term stability tests for monitors of different wavelengths are shown in Figure 4 for some of the more recent field campaigns and PSI laboratory tests. All of the cross-calibration factors in Figure 4 were measured using the particle calibration method. While during some of the campaigns and lab tests cross-calibration factors changed by less than 3% over 20-30 days, during others it varied by up to 15% over similar time periods. The reasons for these different behaviours are not yet fully clear. On the one hand, drifts of the cross-calibration factor were real in some cases, likely caused by contaminations within the detection cell. On the other hand, the precision of the cross-calibration measurements was likely poorer than the actual stability of the instrument. The resulting level of uncertainty in absorption coefficients is greater than acceptable for atmospheric aerosols with a high SSA. As a consequence, it was decided to include further extensive testing of the CAPS PMssa monitor in the work programme of the project "Black Carbon - Metrology for light absorption by atmospheric aerosols" of the European Metrology Programme for Innovation And Research (EMPIR). Preliminary results of this EMPIR Black Carbon project are: (i) refining the calibration procedures substantially improved the reproducibility of the measured cross-calibration factor; (ii) the stability of the cross-calibration factor over several months is sufficient to make accurate absorption coefficient measurements in a long-term monitoring setup potentially possible, if other aspects such as truncation correction are under control (see below).

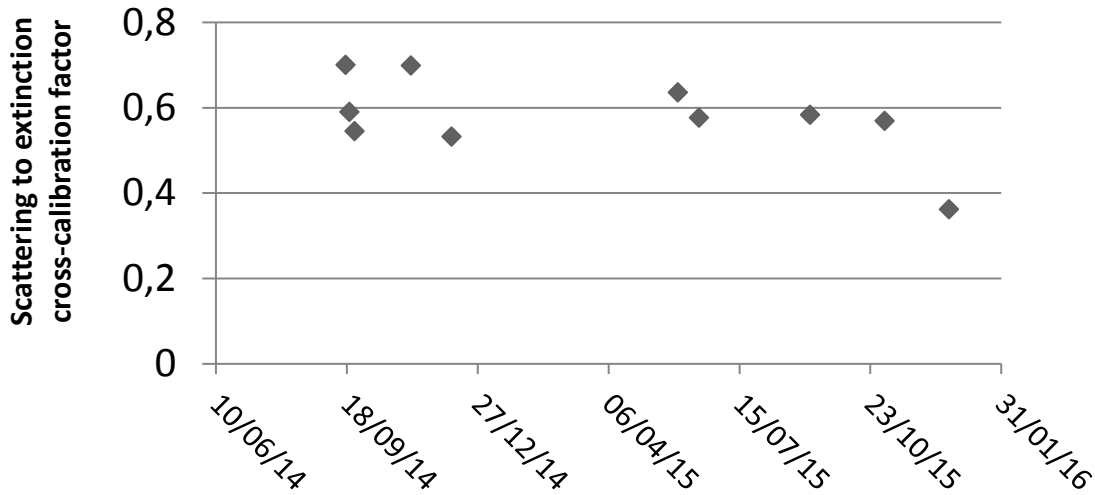


Figure 3: Initial measurements of the 780 nm CAPS PMssa (PSI) scattering to extinction cross-calibration factor. Most likely the precision of these cross-calibration factors is poorer than the actual stability of the instrument.

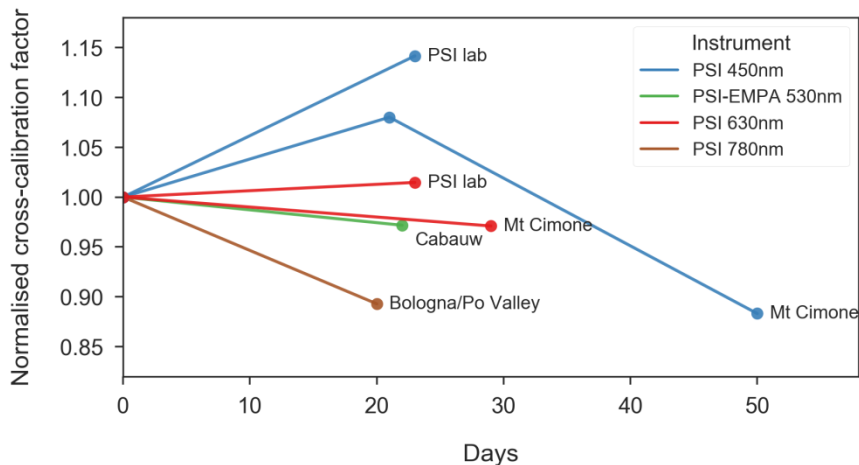


Figure 4: Normalised cross-calibration factors of the PSI CAPS PMssa monitors over the duration of the field campaigns and lab tests indicated in labels on each curve.

2.1.3 Truncation correction of CAPS PMssa scattering coefficients

All types of integrating nephelometers suffer from physical design limitations that prevent the instruments from collecting some fraction of near-forward and near-backward scattered light. This issue is known as scattered light truncation. Particulate scattering coefficients measured with an integrating nephelometer will be systematically biased if truncation is not properly accounted for and corrected. The degree of truncation depends on instrument geometry and the angular distribution of light scattered from the aerosol sample being analysed, also known as the aerosol phase function. Aerosol phase functions depend on particle size distribution, shape, and composition (refractive index).

Given that the phase functions of ambient aerosols are very rarely measured, models are required to calculate phase functions from more commonly measured quantities such as aerosol size distributions in order to perform truncation correction. Such models typically make simplifying assumptions regarding the refractive indices and shapes of the particles being measured. For example particles are commonly

assumed to be spherical and thus treatable with Mie theory. Particles with more complex shapes would require more complex optical models.

Onasch et al., (2015) introduced a Mie-based model for calculating truncation correction factors for the CAPS PM_{ss}a integrating sphere. The model takes as input particle size distribution and complex refractive index. The model was tested against measured scattering truncation values for monodisperse ammonium sulphate. A parameter in the model – the length of the glass tube outside the integrating sphere containing particles that contribute to measured scattering – was adjusted to achieve reasonable closure between the measurements and calculations. The manufacturers of the CAPS have made this model available to users through the software program ‘Mie Amigo’.

The Onasch truncation model did not include a potentially important physical process – reflection of scattered light from the glass tube used to enclose the aerosol flow in the CAPS PM_{ss}a. Such reflection would serve to increase the fraction of scattered light exiting the integrating sphere before being detected, i.e. it would increase truncation. The field deployments of the CAPS PM_{ss}a monitoring during the ACTRIS JRA1 field experiments revealed that uncertainties in the truncation correction are one main limitation for obtaining accurate aerosol absorption coefficients (besides the cross-calibration issue discussed above).

For the above reasons, extensive experimental and theoretical investigation of the light scattering truncation within the CAPS-PM_{ss}a was also included in the work programme of the EMPIR Black Carbon project. PSI developed a new Mie-based truncation model that extended the Onasch model in order to include reflection from the glass tube. Unlike the ‘Mie Amigo’ software, the PSI model can be run in batch processing mode, which is an important feature that enables easy computation of truncation correction factors at high time resolution (e.g. hourly) from size distributions measured during field campaigns that may last for months.

Figure 5 displays truncation curves as a function of particle diameter calculated with both the Onasch and PSI truncation models for a wavelength of 630 nm. As expected, the PSI model including glass tube reflection computes larger truncation values than the Onasch model. The original PSL measurements from Onasch et al., (2015) plus some additional laboratory measurements performed with truly monodisperse particles (classified with an aerodynamic aerosol classifier) in laboratory tests performed at PSI are also displayed on the Figure. It can be seen that: (i) the truncation behaviour of the tested instrument differs from that published in the literature; (ii) neither model is fully consistent with the combined observations. Further work is required to resolve this issue and is currently being performed in the context of the EMPIR Black Carbon project.

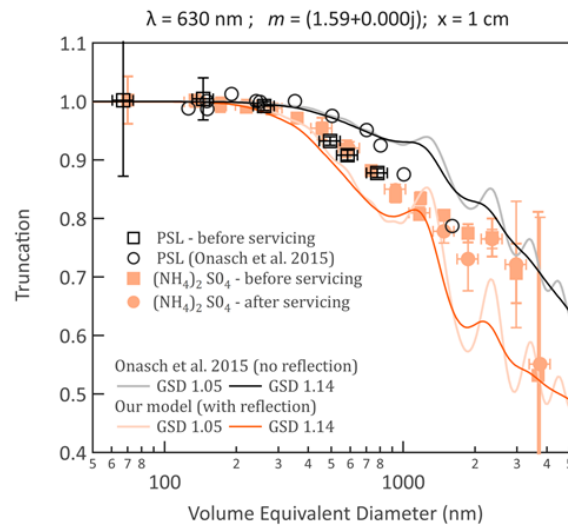


Figure 5: Comparison of measured and modelled truncation values as a function of particle volume equivalent diameter. This figure is a preliminary result of extensive laboratory experiments conducted as a follow-up of the ACTRIS-JRA1 findings in the context of the EMPIR Black Carbon project.

While Figure 5 gives an indication of the differences between different truncation measurements and calculations, it gives no sense of how important these differences might be for the ambient aerosols measured during the field campaigns. To demonstrate this, Figure 6 displays the distributions of the truncation correction factors (the inverse of the ‘truncation’ value plotted in Figure 5) calculated with the PSI truncation model from particle size distributions measured during the Athens, Cabauw and Melpitz winter field campaigns. Calculations were performed both with and without including glass tube reflection in the model. The different types of calculations result in median differences of 5 – 18% in truncation corrections factors for the size distributions measured during these campaigns. This result confirms that further work on truncation models for the CAPS PM_{ss} is required to reduce uncertainties in calculated truncation correction factors for typical particle size distributions measured across Europe.

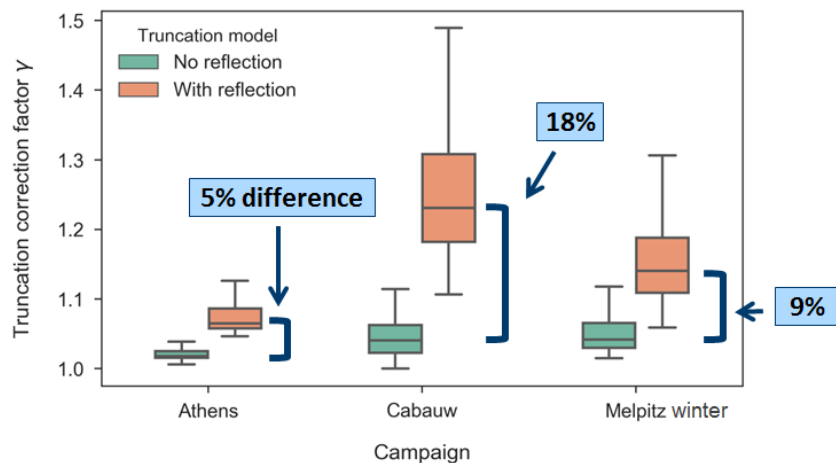


Figure 6: Distributions of the truncation correction factors calculated with the PSI truncation model with and without glass tube reflection included for particle size distributions measured during the Athens, Cabauw, and Melpitz winter field campaigns.

2.1.4 Closure between scattering coefficients measured in the field by CAPS PM_{ss} and other nephelometers

Keeping in mind the quantification issues related to cross-calibration and truncation correction discussed in Sections 2.1.2 and 2.1.3, the performance of the CAPS PM_{ssa} as a nephelometer in the field was assessed by comparing PM_{ssa} scattering coefficients against those measured by independent nephelometers (e.g. TSI 3563, or the Ecotech Aurora 4000) during the field campaigns where both types of data were available. An example result is shown in Figure 7 for hourly-averaged scattering coefficients at two wavelengths measured by CAPS PM_{ssa} (PSI) and an Ecotech Aurora 4000 during the Melpitz summer campaign. Measurements from the two types of nephelometers show excellent correlation and only small biases of 2-4% (slightly larger errors were observed at low scattering coefficients).

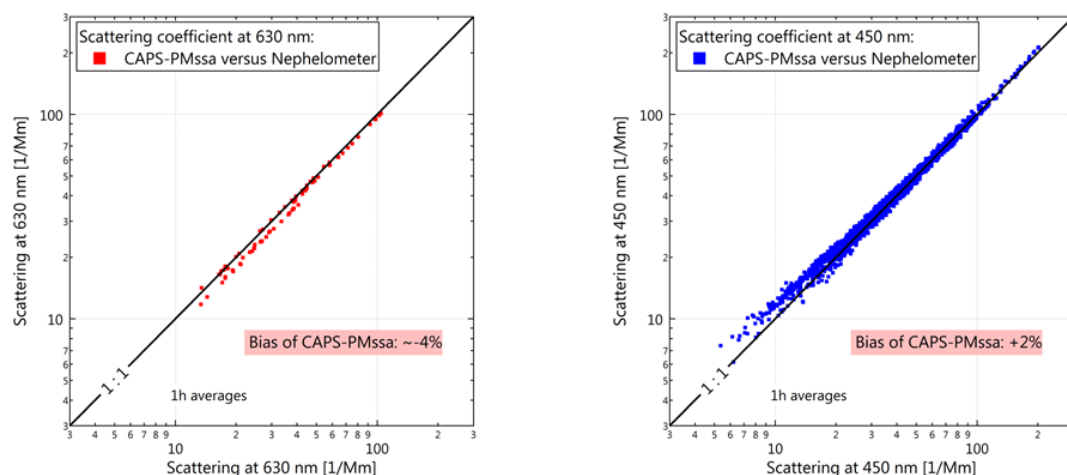


Figure 7: Scattering coefficients measured at 630 and 450 nm by CAPS PM_{ssa} (PSI) and an Ecotech Aurora 4000 (TROPOS) during the Melpitz summer field campaign.

Excellent correlations were also obtained between PM_{ssa} and independent nephelometer measurements during the other field campaigns. However, measurement biases were often larger; e.g. $\sim\pm 15\%$ during the Athens and Cabauw campaigns, only part of which may be attributed to different line losses in the sampling lines. These findings are consistent with our assessment that further work is required on the cross-calibration and truncation correction issues of the CAPS PM_{ssa} to ensure it measures accurate scattering coefficients. If these issues can be properly resolved the CAPS PM_{ssa} shows good promise as a useful, stand-alone nephelometer in the field.

2.1.5 Absolute calibration of CAPS PM_{ssa} extinction coefficients

Extinction in the CAPS PM_{ssa} is measured by cavity attenuated phase shift spectroscopy (Kebabian et al., 2007). An important potential source of systematic bias in measured extinction is the 'geometry correction factor', k . This factor corrects for the increase in optical path length in the optical cavity of the CAPS PM_{ssa} due to the particle-free purge air flows that are required to prevent contamination of the very high reflectivity cavity mirrors. The default value for k set by the CAPS PM_{ssa} manufacturer Aerodyne, Inc. is 1.37. This value was determined in a single experiment where Mie-calculated and measured extinction cross-sections were compared for PSL particles (Onasch et al., 2015). The k value of the CAPS PM_{ex} (the extinction-only instrument that was the precursor to the CAPS PM_{ssa}) was measured as 1.27 in a similar type of experiment (Petzold et al., 2013a). Differences in the PM_{ex} and PM_{ssa} k values are due to differences in cavity geometries between these two instruments.

The stability of the CAPS k value was investigated with a series of absolute calibration experiments performed at TROPOS over a period of almost one year as part of the EMPIR Black Carbon project. The experiments were performed with three TROPOS CAPS PM_{ex} monitors operating at wavelengths of 450, 530, and 660 nm. Extinction values of non-absorbing ammonium sulphate aerosols were measured with the three PM_{ex} monitors and a reference integrating nephelometer (Ecotech Aurora 4000; Müller et al., 2011b). The reference nephelometer was calibrated with CO₂ before each experiment and corrected for

truncation with measured scattering Ångstrom exponents. PMex correction factors were determined as the slopes of linear fits between the PMex and reference nephelometer measurements. The errors of the fits were very small (<0.13%). The correction factors for each PMex monitor were very stable, varying by less than 3% around the mean for each instrument over the period of almost 1 year. This indicates that the k values and – more generally – the b_{ext} measurements performed by the CAPS monitors are stable over time, which is an essential condition for the CAPS PMssa monitors to be able to perform useful absorption measurements over an extended period of time.

The TROPOS experiments also indicated that while stable, CAPS extinction measurements need to be calibrated against an accepted reference standard (e.g. scattering coefficients of non-absorbing particles measured by a CO₂-calibrated nephelometer). This is likely because the geometry correction factors of individual CAPS monitors differ from the default factory values set by Aerodyne (1.37 for the PMssa, 1.27 for the PMex). We recommend that these absolute extinction calibrations be performed in the absorption photometer workshops performed at the European Center for Aerosol Calibration (ECAC). The three CAPS PMssa monitors from PSI participated in the January 2017 ECAC workshop (AP-2017-1). Extinction values measured by the 450, 630, and 780 nm PMssa monitors were 12%, 1%, and 12% higher, respectively, than values measured by the reference measurement. This corresponds to effective k values of 1.21, 1.36, and 1.21, respectively.

2.1.6 Closure between extinction coefficients measured in the field by CAPS PMssa and other instruments

Extinction values measured by the CAPS PMssa and PMex are generally consistent (Figure 8). Biases might be due to incorrectly set geometry correction factors (Section 2.1.5) or non-linear behaviour when the mirrors of the CAPS cavity become contaminated. The latter was indeed observed during the Melpitz summer campaign, when one of two CAPS monitors operating at equal wavelength got contaminated in two steps (450 nm monitors Figure 8). This is another reason why regular calibration of the CAPS extinction channel at the ECAC calibration centre is required.

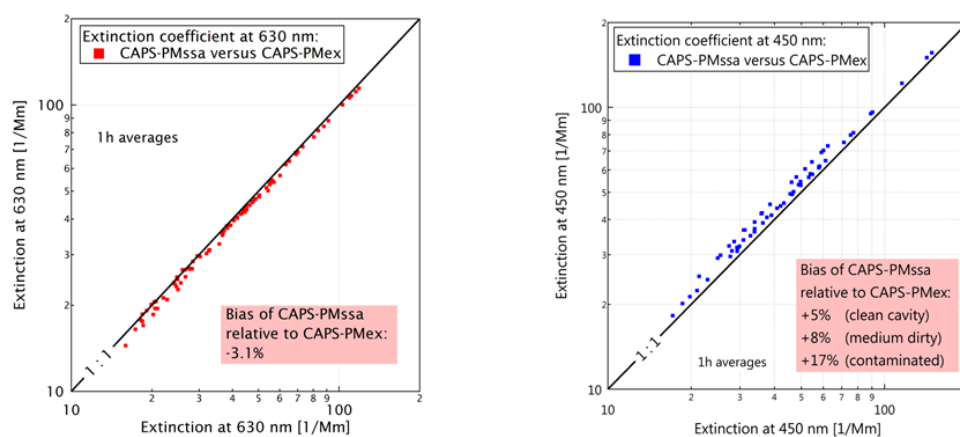


Figure 8: Extinction coefficients measured at (a) 630 and (b) 450 nm by CAPS PMssa (PSI) and CAPS PMex (TROPOS) during the Melpitz summer field campaign.

Extinction values measured by CAPS PMssa were also consistent with extinction values calculated as the sum of scattering measured with a TSI 3563 nephelometer and absorption measured with a MAAP during the Cabauw campaign. As SSA values generally fell in the range 0.8 to 0.9 during this campaign, this agreement is consistent with the excellent correlation observed between scattering coefficients measured by CAPS PMssa and the TSI nephelometer and between the scattering and extinction channels of the PMssa (good cross-calibration).

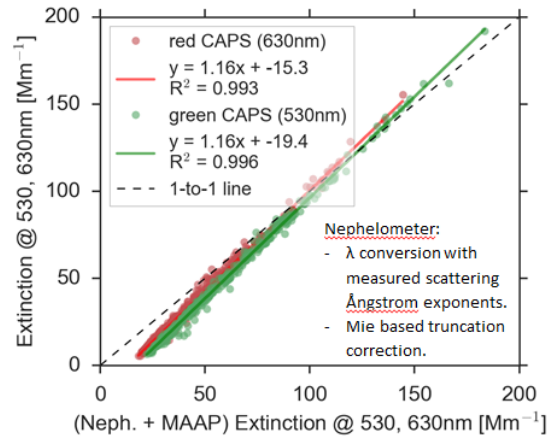


Figure 9: Extinction coefficients measured at 530 and 630 nm by CAPS PMSSa (PSI) compared to extinction coefficients derived from the sum of scattering measured with a TSI 3563 nephelometer (KNMI, TNO) and absorption measured with a MAAP (KNMI, TNO) during the Cabauw field campaign.

2.1.7 Closure between absorption coefficients measured in the field by CAPS PMSSa and other instruments

The MAAP proved to be a stable and reliable instrument throughout all field campaigns. Therefore, in the absence of a traceable or standard absorption reference measurement, we used absorption coefficients measured by the MAAP to assess the performance of the CAPS PMSSa as an absorption photometer. Figure 10 displays a typical example of an absorption coefficient time series measured over approximately one month during the Cabauw field campaign. Hourly-averaged absorption coefficients measured by 530 and 630 nm PMSSa monitors (PSI; no truncation correction applied) and a MAAP (KNMI/TNO) are shown. Good correlation is observed between the coefficients measured by each instrument demonstrating that the CAPS PMSSa is able to run stably over the period of an intensive field campaign.

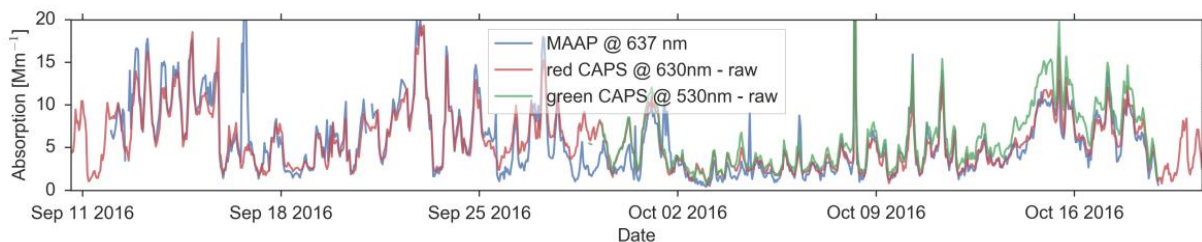


Figure 10: Cabauw example, raw absorption coefficient measurements of CAPS-PMSSa at 630 nm and at 530 nm compared to MAAP at 637 nm

To investigate quantitative performance more closely scatter plots of PMSSa absorption coefficients against those measured by MAAP instruments are displayed in Figures Figure 11 and Figure 12 for the Athens and Bologna (San Pietro Capofiume site) field campaigns. Absolute biases between the different instruments remain that are most likely related to cross-calibration and truncation correction of the PMSSa monitors. The apparent limits of absorption coefficient quantification for the PMSSa monitors were ~ 5 and ~ 0.6 Mm⁻¹ in the Athens and Bologna campaigns, respectively.

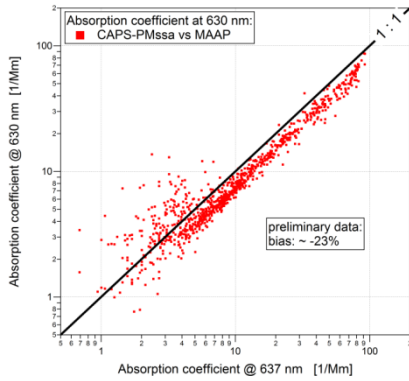


Figure 11: Athens example, raw absorption coefficient measurements of CAPS-PMssa at 630 nm compared to MAAP at 637 nm.

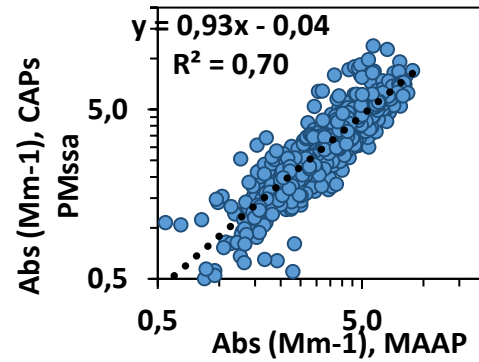


Figure 12: San Pietro Capofiume (Bologna campaign) example, raw absorption coefficient measurements of CAPS-PMssa at 630 nm compared to MAAP at 637 nm.

The measurements at 630 nm from the Cabauw campaign were used to assess the hypothesis that biases between PMssa and MAAP measurements were predominantly related to the correction factors applied to the PMssa measurements (cross-calibration, truncation correction and/or geometry correction). The results of this assessment are displayed in Figure 13. Correcting the PMssa measurements for truncation clearly worsened the comparison between the two measurements (middle Figure panel). In particular, an SSA dependent bias was introduced to the level of disagreement between PMssa and MAAP. Assuming that absorption coefficients measured by both instruments should not systematically depend on SSA, the CAPS PMssa scattering coefficients were tweaked by a constant value to minimize systematic dependence of deviation on SSA. As well as removing the SSA bias (by design), this process improved the level of agreement between the absorption coefficients measured by the CAPS PMssa and MAAP. This exercise provides hope that once the PMssa correction factors can be adequately determined in an independent manner (i.e. without co-located MAAP measurements), the instrument will prove to be a useful, stand-alone field absorption photometer.

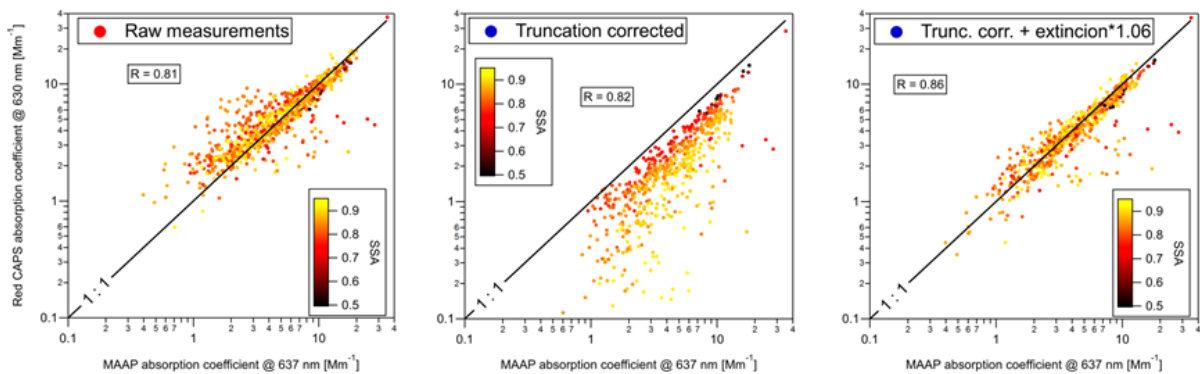


Figure 13: Cabauw example of absorption coefficient measurements by CAPS PMssa at 630 nm and MAAP at 637 nm. It is shown that ‘tweaking’ of the CAPS PMssa correction factors to minimize any systematic SSA-dependent bias relative to MAAP measurements improves the quantitative agreement between the two measurements.

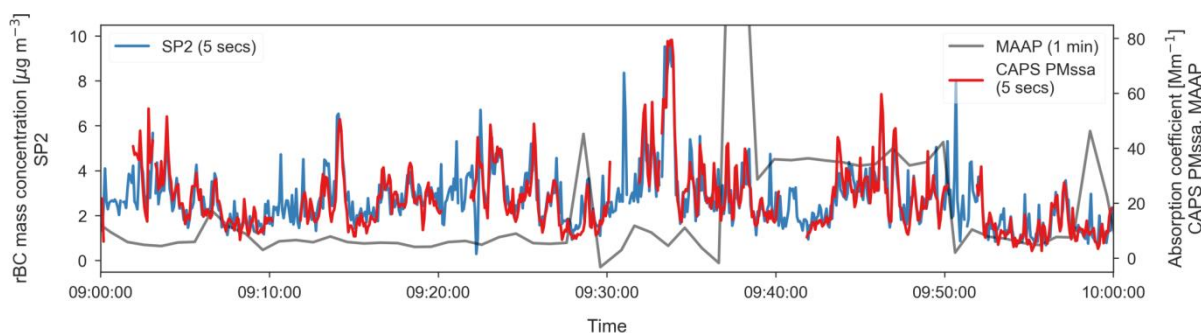


Figure 14: Mobile measurements of absorption coefficients (MAAP at 637 nm and CAPS PMssa at 780 nm) and rBC mass concentrations (SP2) performed in the PSI mobile measurements van along a stretch of highway in the Po Valley (Bologna campaign).

A key advantage of moving beyond filter-based absorption photometers such as the MAAP is to increase measurement sensitivity and time resolution. This point is illustrated in Figure 14, which displays absorption coefficients measured by MAAP (at 637 nm) and CAPS PMssa (at 780 nm) and rBC mass concentrations measured by SP2 from the PSI mobile measurements van during the Bologna field campaign. Although the absolute levels still require correction, the PMssa absorption coefficients correlate extremely well with the rBC mass concentrations at a time resolution of 5 secs. Peaks in both time series correspond to plumes from passing vehicles on the highway. This example demonstrates that both the SP2 and CAPS PMssa are capable of measuring with excellent time resolution. By contrast, the MAAP is not designed to operate at such high time resolution and its measurements do not follow the other two time series.

2.2 The photoacoustic extinciometer (PAX)

2.2.1 Description of the instrument

A photoacoustic extinciometer (PAX) was deployed during the winter campaign in Melpitz, in addition to the instrumentation originally foreseen for the ACTRIS JRA1 activities. While detailed assessment of calibration procedures and instrument performance is the topic of other projects, we still provide some first results here, as photoacoustic measurements also have the potential to become suitable for long-term operation at ACTRIS observatories in the near or medium future.

2.2.2 Closure between absorption coefficients measured in the field by the PAX and other instruments

Absorption coefficients measured by the PAX at 870 nm are compared against MAAP absorption coefficients at 637 nm at three different time resolutions in Figure 15. Excellent correlation between the two types of measurements was observed. This is remarkable considering the fact that the two measurement methods – *in situ* and filter-based detection – are very different, and suffer from different types of measurement artefacts. This suggests that the measurement artefacts for both instruments are likely small. An AAE value of 2.7 was required to bring the two types of measurements done at different wavelengths into quantitative agreement. However, it should be noted that the calibration of the PAX measurements is still being investigated and this value might change.

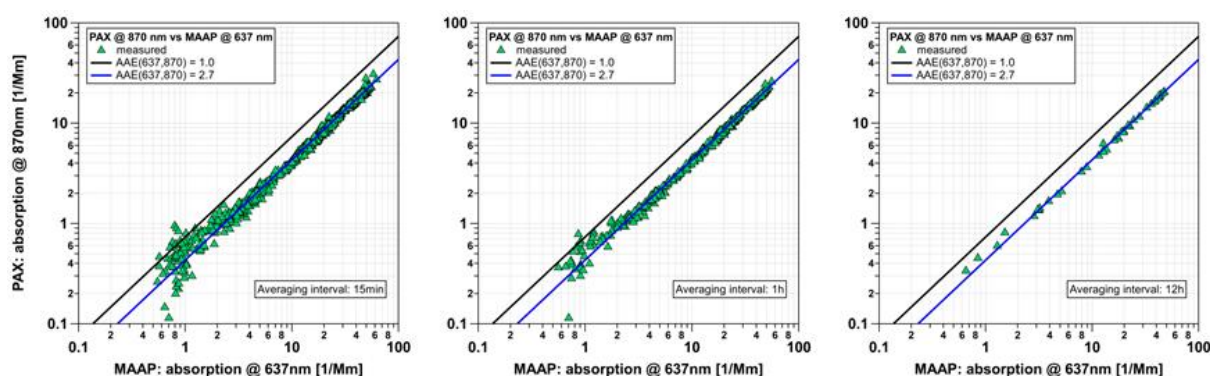


Figure 15: Melpitz winter campaign example, absorption coefficient measurements of PAX at 870 nm compared to MAAP at 637 nm.

2.3 Summary of ambient absorption coefficients and outlook for the future

There is no standard reference technique for measuring atmospheric aerosol absorption coefficients, nor a standard reference material with which to calibrate absorption photometers. Throughout the field campaigns conducted for JRA1 Task 11.1, the MAAP proved – at least – to be a useful, stable and reliable reference point for comparing absorption coefficients measured at different sites and during different campaigns. Unfortunately production of the MAAP was discontinued in 2017. Additionally, there is strong motivation to leverage new technologies (e.g. CAPS) and move beyond filter-based absorption photometers to avoid measurement artefacts due to the interaction of light with the filter material itself, and to achieve higher sensitivities in order to perform high time resolution measurements (e.g. Figure 14). The CAPS PM_{ss} isn't quite ready for independent reliable absorption coefficient measurements; however, the latest progress in lab studies conducted in the EMPIR Black Carbon project suggests that this may soon be the case.

3 BC mass concentration results

3.1 Closure between BC mass concentrations measured in the field by the SP2 and thermal-optical methods

BC mass has traditionally been detected as EC measured by thermal-optical evolved gas analysis. This remains the analytical method of choice in monitoring networks. More recently, campaign-based SP2 measurements of rBC mass concentrations have become more common and used to represent BC mass concentrations in the atmosphere. Given both methods detect the operationally defined quantities EC and rBC as discussed in the Introduction section 1, differences between the two quantities are to be expected due to aerosol-dependent calibration biases and measurement artefacts.

rBC mass concentrations measured by SP2 are compared with EC mass concentrations measured by the EUSAAR2 thermal-optical protocol in Figures Figure 16 Figure 17 Figure 18, and Figure 19 for the Melpitz summer, Melpitz winter, Cabauw, and Bologna field campaigns, respectively. Reasonable correlation was generally observed between the two quantities, indicating that both methods respond effectively and similarly to BC mass. However, quantitative agreement between the two quantities was more variable and less promising. The slopes of linear fits to the scatter plots ranged from 0.5 to 2. During the Cabauw and Bologna campaigns, rBC concentrations were lower than corresponding EC concentrations. The reasons for these discrepancies are not yet clear and difficult or impossible to determine without an absolute reference standard for BC. On the other hand, SP2 concentrations were on average a factor of two higher than EC concentrations during the Melpitz winter campaign. This was likely due to overloading of the EC filters during the high concentrations periods encountered during that campaign. Filter overloading can interfere with the optical detection of pyrolytic carbon, leading to systematic bias in reported EC concentrations.

Given the range of discrepancies observed between rBC and EC concentrations in these campaigns, future studies – including monitoring-based activities – would ideally measure both of these quantities, in order to explore possible systematic biases that might otherwise go undetected. Operation of the SP2 would bring the additional advantage of very high time resolution (e.g. Figure 14) rBC mass concentration measurements, which would open up the possibility of studying MAC_{BC} on very short timescales. However, the original SP2 is not suitable for long-term measurements as it is too demanding in terms of both operation and data processing.

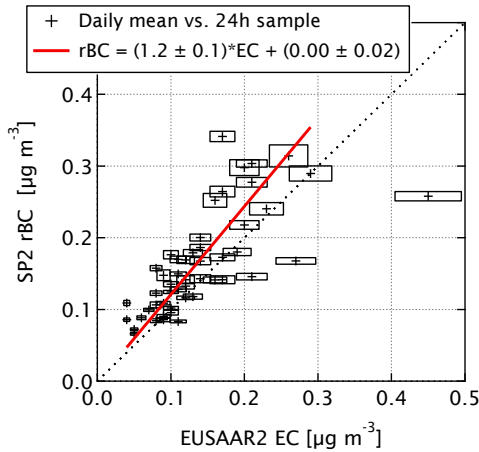


Figure 16: Melpitz summer rBC mass concentrations measured by SP2 and EC mass concentrations measured with the EUSAAR2 thermal-optical protocol.

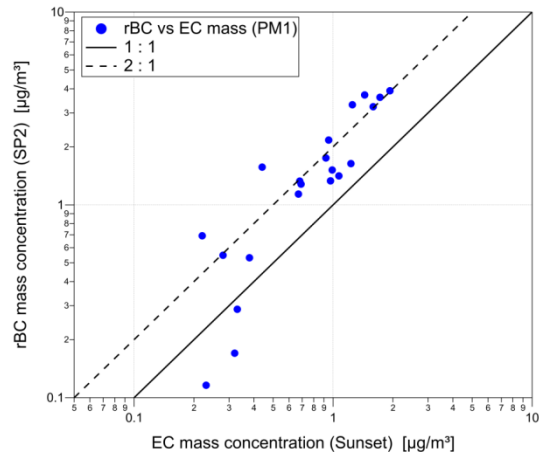


Figure 17: Melpitz winter rBC mass concentrations measured by SP2 and EC mass concentrations measured with the EUSAAR2 thermal-optical protocol.

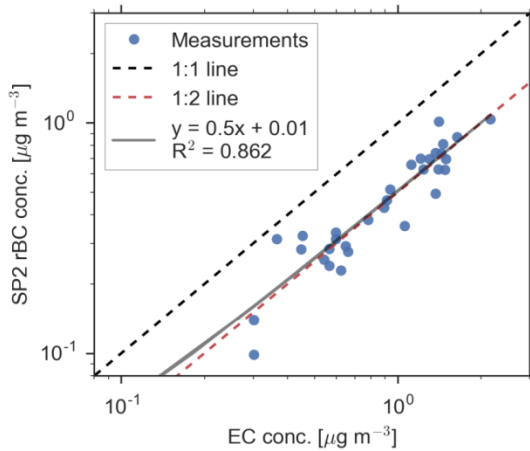


Figure 18: Cabauw rBC mass concentrations measured by SP2 and EC mass concentrations measured with the EUSAAR2 thermal-optical protocol.

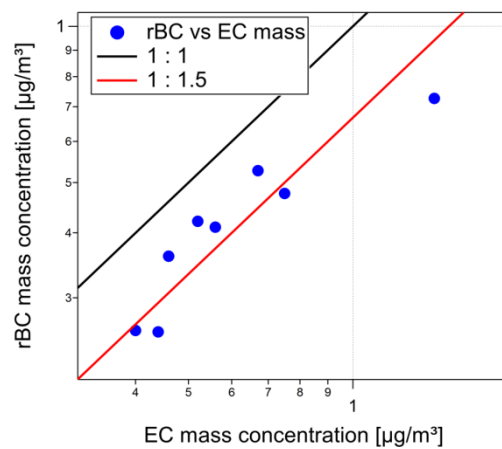


Figure 19: Bologna rBC mass concentrations measured by SP2 and EC mass concentrations measured with the EUSAAR2 thermal-optical protocol.

3.2 The next generation SP2 instrument: the extended range SP2 (SP2-XR)

Very recently a compact and simplified version of the SP2 was developed – the SP2-XR. In contrast to the original SP2, the SP2-XR is much easier to operate, creating the potential for long-term unattended operation. An SP2-XR was deployed during the winter campaign in Melpitz, in addition to the instrumentation originally foreseen for the ACTRIS JRA1 activities. The data processing procedures for

the new SP2-XR instrument are still under development and consequently the measurements over the full campaign have not been processed yet. Here we present rBC mass concentrations and mass size distributions measured by the SP2-XR over only a single night at the beginning of the campaign. They are compared to the corresponding SP2 measurements in Figure 20. Given the SP2-XR data processing is still a work in progress the agreement between the two instruments is very promising with respect to both rBC mass concentrations and size distributions.

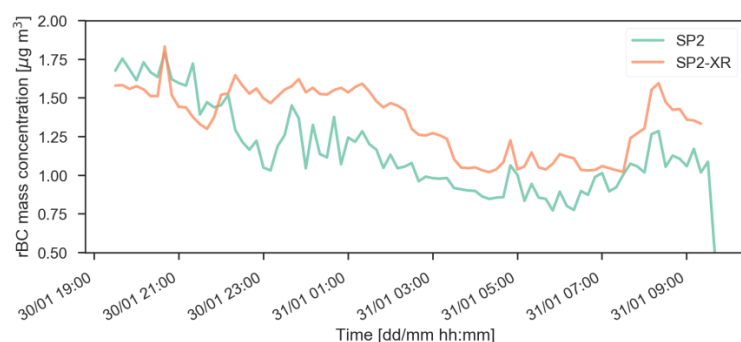


Figure 20: rBC mass concentrations measured by SP2 and SP2-XR overnight in Leipzig (TROPOS) before the beginning of the Melpitz winter campaign. Note the SP2 signal has relatively high random noise as the data were acquired with an under-sampling factor of 200.

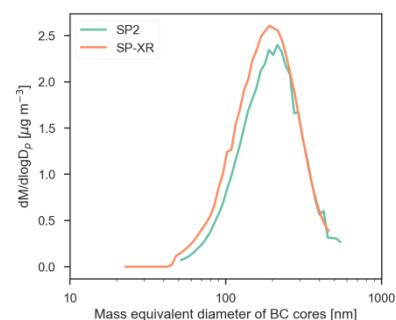


Figure 21: Average rBC mass size distributions measured by SP2 and SP2-XR overnight in Leipzig (TROPOS) before the beginning of the Melpitz winter campaign.

4 Outlook: MAC_{BC} measurements

Often in field campaigns only one measurement of absorption coefficient and one measurement of BC mass concentration is performed and then used to calculate MAC_{BC} values. The JRA1 campaigns allowed comprehensive intercomparison of a number of different methods used to measure these two quantities directly in the field. The results demonstrated that in the absence of absolute reference standards for both aerosol absorption and BC mass, the intercomparison of different methods is a critical process. While measurements by the investigated methods generally showed good to excellent correlation between themselves, systematic biases were often detected. These biases might easily have gone undetected without the benefit of the co-located measurements. Biases in absorption coefficients and BC mass measurements feed directly into the calculation of MAC_{BC} values. Therefore, it is important to identify and understand these biases before interpreting MAC_{BC} variability over time or before comparing absolute MAC_{BC} values measured in different studies.

A number of the critical issues that were identified in this work package are already being addressed in follow up projects. For example based on the results shown in Sections 2.1.2, 2.1.3, and 2.1.5, further and extensive laboratory studies are being performed for the EMPIR Black Carbon project at PSI and TROPOS to more accurately characterise the cross-calibration, truncation correction, and geometry correction factors for the CAPS PM_{ss}. If these goals can be achieved, the CAPS PM_{ss} has the potential to be a useful field-based absorption photometer, at least over the durations of typical intensive field campaigns. On the BC mass side, PSI and AWI are conducting further measurements to assess the capability of the SP2-XR as a monitoring instrument that could potentially be used to compliment the EC concentration measurements currently performed in the ACTRIS network.

5 References

- Anderson, T. I., Covert, D. S., Marshall, S. F., Laucks, M. I., Charlson, R. J., Waggoner, A. P., Ogren, J. A., Caldow, R., Holm, R. I., Quant, F. R., Sem, G. J., Wiedensohler, A., Ahlquist, N. A. and Bates, T. S.: Performance Characteristics of a High-Sensitivity, Three-Wavelength, Total Scatter/Backscatter Nephelometer, *J. Atmospheric Ocean. Technol.*, 13(5), 967–986, doi:10.1175/1520-0426(1996)013<0967:PCOAHS>2.0.CO;2, 1996.
- Babu, S. S., Moorthy, K. K., Manchanda, R. K., Sinha, P. R., Satheesh, S. K., Vajja, D. P., Srinivasan, S. and Kumar, V. H. A.: Free tropospheric black carbon aerosol measurements using high altitude balloon: Do BC layers build “their own homes” up in the atmosphere?, *Geophys. Res. Lett.*, 38(8), doi:10.1029/2011GL046654, 2011.
- Bond, T. C., Doherty, S. J., Fahey, D. W., Forster, P. M., Berntsen, T., DeAngelo, B. J., Flanner, M. G., Ghan, S., Kärcher, B., Koch, D., Kinne, S., Kondo, Y., Quinn, P. K., Sarofim, M. C., Schultz, M. G., Schulz, M., Venkataraman, C., Zhang, H., Zhang, S., Bellouin, N., Guttikunda, S. K., Hopke, P. K., Jacobson, M. Z., Kaiser, J. W., Klimont, Z., Lohmann, U., Schwarz, J. P., Shindell, D., Storelmo, T., Warren, S. G. and Zender, C. S.: Bounding the role of black carbon in the climate system: A scientific assessment, *J. Geophys. Res. Atmospheres*, 118(11), 5380–5552, doi:10.1002/jgrd.50171, 2013.
- Cavalli, F., Viana, M., Yttri, K. E., Genberg, J. and Putaud, J.-P.: Toward a standardised thermal-optical protocol for measuring atmospheric organic and elemental carbon: the EUSAAR protocol, *Atmospheric Meas. Tech.*, 3(1), 79–89, doi:https://doi.org/10.5194/amt-3-79-2010, 2010.
- Drinovec, L., Močnik, G., Zotter, P., Prévôt, A. S. H., Ruckstuhl, C., Coz, E., Rupakheti, M., Sciare, J., Müller, T., Wiedensohler, A. and Hansen, A. D. A.: The “dual-spot” Aethalometer: an improved measurement of aerosol black carbon with real-time loading compensation, *Atmos Meas Tech*, 8(5), 1965–1979, doi:10.5194/amt-8-1965-2015, 2015.
- IPCC: Summary for Policymakers. In: *Climate Change 2013: The Physical Science Basis. Contribution of Working Group I to the Fifth Assessment Report of the Intergovernmental Panel on Climate Change* [Stocker, T.F., D. Qin, G.-K. Plattner, M. Tignor, S.K. Allen, J. Boschung, A. Nauels, Y. Xia, V. Bex and P.M. Midgley (eds.)], Cambridge University Press, Cambridge, United Kingdom and New York, NY, USA., 2013.
- Kebabian, P. L., Robinson, W. A. and Freedman, A.: Optical extinction monitor using cw cavity enhanced detection, *Rev. Sci. Instrum.*, 78(6), 063102, doi:10.1063/1.2744223, 2007.
- Laborde, M., Mertes, P., Zieger, P., Dommen, J., Baltensperger, U. and Gysel, M.: Sensitivity of the Single Particle Soot Photometer to different black carbon types, *Atmos Meas Tech*, 5(5), 1031–1043, doi:10.5194/amt-5-1031-2012, 2012.
- Loeb, N. G. and Su, W.: Direct Aerosol Radiative Forcing Uncertainty Based on a Radiative Perturbation Analysis, *J. Clim.*, 23(19), 5288–5293, doi:10.1175/2010JCLI3543.1, 2010.
- Massoli, P., Kebabian, P. L., Onasch, T. B., Hills, F. B. and Freedman, A.: Aerosol Light Extinction Measurements by Cavity Attenuated Phase Shift (CAPS) Spectroscopy: Laboratory Validation and Field Deployment of a Compact Aerosol Particle Extinction Monitor, *Aerosol Sci. Technol.*, 44(6), 428–435, doi:10.1080/02786821003716599, 2010.
- Moteki, N. and Kondo, Y.: Effects of Mixing State on Black Carbon Measurements by Laser-Induced Incandescence, *Aerosol Sci. Technol.*, 41(4), 398–417, doi:10.1080/02786820701199728, 2007.

Müller, T., Henzing, J. S., de Leeuw, G., Wiedensohler, A., Alastuey, A., Angelov, H., Bizjak, M., Collaud Coen, M., Engström, J. E., Gruening, C., Hillamo, R., Hoffer, A., Imre, K., Ivanow, P., Jennings, G., Sun, J. Y., Kalivitis, N., Karlsson, H., Komppula, M., Laj, P., Li, S.-M., Lunder, C., Marinoni, A., Martins dos Santos, S., Moerman, M., Nowak, A., Ogren, J. A., Petzold, A., Pichon, J. M., Rodriguez, S., Sharma, S., Sheridan, P. J., Teinilä, K., Tuch, T., Viana, M., Virkkula, A., Weingartner, E., Wilhelm, R. and Wang, Y. Q.: Characterization and intercomparison of aerosol absorption photometers: result of two intercomparison workshops, *Atmos Meas Tech*, 4(2), 245–268, doi:10.5194/amt-4-245-2011, 2011a.

Müller, T., Laborde, M., Kassell, G. and Wiedensohler, A.: Design and performance of a three-wavelength LED-based total scatter and backscatter integrating nephelometer, *Atmos Meas Tech*, 4(6), 1291–1303, doi:10.5194/amt-4-1291-2011, 2011b.

Onasch, T. B., Massoli, P., Kehejian, P. L., Hills, F. B., Bacon, F. W. and Freedman, A.: Single Scattering Albedo Monitor for Airborne Particulates, *Aerosol Sci. Technol.*, 49(4), 267–279, doi:10.1080/02786826.2015.1022248, 2015.

Petzold, A. and Schönlinner, M.: Multi-angle absorption photometry—a new method for the measurement of aerosol light absorption and atmospheric black carbon, *J. Aerosol Sci.*, 35(4), 421–441, doi:10.1016/j.jaerosci.2003.09.005, 2004.

Petzold, A., Rasp, K., Weinzierl, B., Esselborn, M., Hamburger, T., Dörnbrack, A., Kandler, K., Schütz, L., Knippertz, P., Fiebig, M. and Virkkula, A.: Saharan dust absorption and refractive index from aircraft-based observations during SAMUM 2006, *Tellus B*, 61(1), 118–130, doi:10.1111/j.1600-0889.2008.00383.x, 2009.

Petzold, A., Onasch, T., Kehejian, P. and Freedman, A.: Intercomparison of a Cavity Attenuated Phase Shift-based extinction monitor (CAPS PMex) with an integrating nephelometer and a filter-based absorption monitor, *Atmos Meas Tech*, 6(5), 1141–1151, doi:10.5194/amt-6-1141-2013, 2013a.

Petzold, A., Ogren, J. A., Fiebig, M., Laj, P., Li, S.-M., Baltensperger, U., Holzer-Popp, T., Kinne, S., Pappalardo, G., Sugimoto, N., Wehrli, C., Wiedensohler, A. and Zhang, X.-Y.: Recommendations for reporting “black carbon” measurements, *Atmos Chem Phys*, 13(16), 8365–8379, doi:10.5194/acp-13-8365-2013, 2013b.

Schwarz, J. P., Spackman, J. R., Gao, R. S., Perring, A. E., Cross, E., Onasch, T. B., Ahern, A., Wrobel, W., Davidovits, P., Olfert, J., Dubey, M. K., Mazzoleni, C. and Fahey, D. W.: The Detection Efficiency of the Single Particle Soot Photometer, *Aerosol Sci. Technol.*, 44(8), 612–628, doi:10.1080/02786826.2010.481298, 2010.

Slowik, J. G., Cross, E. S., Han, J.-H., Davidovits, P., Onasch, T. B., Jayne, J. T., Williams, L. R., Canagaratna, M. R., Worsnop, D. R., Chakrabarty, R. K., Moosmüller, H., Arnott, W. P., Schwarz, J. P., Gao, R.-S., Fahey, D. W., Kok, G. L. and Petzold, A.: An Inter-Comparison of Instruments Measuring Black Carbon Content of Soot Particles, *Aerosol Sci. Technol.*, 41(3), 295–314, doi:10.1080/02786820701197078, 2007.

Zarzycki, C. M. and Bond, T. C.: How much can the vertical distribution of black carbon affect its global direct radiative forcing?, *Geophys. Res. Lett.*, 37, L20807, doi:10.1029/2010gl044555, 2010.